Atmos. Meas. Tech. Discuss., doi:10.5194/amt-2016-139, 2016
Manuscript under review for journal Atmos. Meas. Tech.
Published: 3 June 2016

Atmospheric Measurement Techniques Discussions

Trends of tropical tropospheric ozone from twenty years of European satellite measurements and perspectives for Sentinel-5 Precursor

Heue Klaus-Peter[1], Coldewey-Egbers Melanie[1], Delcloo Andy[2], Lerot Christophe[3], Loyola Diego[1], Valks Pieter[1], and van Roozendael Michel[3]

[1]Deutsches Zentrum für Luft- und Raumfahrt, Münchener Strasse 20, 82234 Oberpfaffenhofen
[2]Royal Meteorological Institute, Avenue Circulaire 3, 1180 Brussels
[3]Royal Belgian Institute for Space Aeronomy, Ringlaan 3, 1180 Brussels

Correspondence to: klaus-peter.heue@dlr.de

Abstract. In preparation of the TROPOMI/S5P launch in autumn 2016 a tropospheric ozone retrieval based on the convective cloud differential method was developed. For intensive tests we applied the algorithm to the total ozone columns and cloud data of the satellites GOME, SCIAMACHY, OMI, GOME-2A and GOME-2B. Thereby a time series of 20 years (1995-2015) of tropospheric ozone columns was retrieved. To have a consistent total ozone data set for all sensors one common retrieval algorithm, namely GODFITv3, has been applied to all sensors and the L1 reflectances have also been soft calibrated. These data were input into the tropospheric ozone retrieval. However, the Tropical Tropospheric Ozone Columns (TTOC) for the individual instruments still showed small differences and therefore we harmonised the data set. For this purpose a multivariant function was fitted to the averaged difference between SCIAMACHY's TTOC and those from the other sensors. The original TTOC was corrected by the fitted offset. GOME-2B data were corrected relative to the harmonised data from OMI and GOME-2A. The harmonisation leads to a better agreement between the different instruments. Also a direct comparison of the TTOCs in the overlapping periods proves that GOME-2A agrees much better with SCIAMACHY after the harmonisation. The improvements for OMI were small. The GOME and SCIAMACHY data overlap for one year for the complete tropics, this turned out to be insufficient to extrapolate back until 1995.

Based on the harmonised observations, we created a merged data product, containing the TTOC from July 1995 to Dec. 2015. A first application of this 20 years record is a trend analysis. The global tropical trend is $0.75 \pm 0.12\,\mathrm{DU\,decade^{-1}}$. Regionally the trends reaches up to $1.8\,\mathrm{DU\,decade^{-1}}$ like on the African Atlantic coast, over the Western Pacific the tropospheric ozone declined over the last 20 years with up to $0.8\,\mathrm{DU\,decade^{-1}}$. The tropical tropospheric data record will be extended in the future with the TROPOMI/S5P data, where the TTOC is part of the operational products.

Atmos. Meas. Tech. Discuss., doi:10.5194/amt-2016-139, 2016
Manuscript under review for journal Atmos. Meas. Tech.
Published: 3 June 2016

Atmospheric Measurement Techniques Discussions

1 Introduction

Tropospheric ozone is a greenhouse gas and has at least locally doubled in the last 50 years (Cooper et al., 2014). Moreover ozone is harmful to humans (Nawrot et al., 2006) and plants. According to Feng and Kobayashi (2009) it is responsible for 5% to 20% crop loss.

The main sources of ozone in troposphere are stratospheric intrusions resulting in a downward transport of stratospheric ozone into the troposphere and photochemical production in the troposphere. The first source is important especially close to the subtropical jet streams (20°-30° south or north). The photochemical source depends on the availability of the ozone precursors and the incident sunlight. In the atmosphere NO_2 is photo dissociated to NO and O^*, the atomic oxygen reacts in a three body process with molecular oxygen and forms O_3.

$$NO_2 \xrightarrow{h\nu} NO + O^* \tag{R1}$$

$$O^* + O_2 \xrightarrow{M} O_3. \tag{R2}$$

On the other hand ozone is destroyed by the reaction with nitrogen monoxide:

$$NO + O_3 \rightarrow NO_2 + O_2 \tag{R3}$$

These reactions lead to the photo-stationary Leighton ratio

$$L = \frac{NO}{NO_2} = \frac{J_{R1}}{O_3 \cdot k_{R3}}. \tag{1}$$

Thereby ozone is neither destroyed nor built, but as soon as other oxidising species (peroxy radicals) are involved, the reaction R3 is replaced and the ozone concentration increases. The reaction of VOCs (volatile organic compounds) with the OH radicals are the main source of the peroxy radicals HO_2 or RO_2. In the end the ozone concentration can be limited by a lack of VOCs or a lack of nitrogen oxides. The first case is often the observed in the city centers where the $NO_x (= NO + NO_2)$ concentration is high. In this case an increase in NO_x reduces the local ozone concentration. Downwind of the center in the suburbs, VOCs are mixed in and the ozone concentration may reach hazardous levels. The second case of a NO_x limited regime can be found in remote areas or over oceans where NO_x concentrations can be extremely low. The chemical sinks are photolysis or the reaction with halogen compounds e.g. ClO or with some VOCs with double bounds e.g. isoprene, in the troposphere also surface deposition is an important sink.

Fishman and Larsen (1987) derived first implication for tropospheric ozone from TOMS (Total Ozone mapping spectrometer) and Stratospheric Aerosol and Gas Experiment (SAGE) ozone profile data, by applying a tropospheric ozone residual technique. Other approaches to derive the tropospheric ozone column from satellites were developed. Many of them rely on the residual technique where the stratospheric column is subtracted from the total column. In the convective cloud differential (CCD) method both the stratospheric and the total column product are derived from the same satellite data. The stratospheric

Atmos. Meas. Tech. Discuss., doi:10.5194/amt-2016-139, 2016
Manuscript under review for journal Atmos. Meas. Tech.
Published: 3 June 2016

Atmospheric Measurement Techniques Discussions

column is estimated based on the ozone column above high reaching convective clouds, which shield the tropospheric ozone. For cloud free observation on the other hand the troposphere is included in the total column. This method was first applied to Total Ozone Mapping Spectrometer (TOMS) data by Ziemke et al. (1998).

In Europe and the US ozone reduction efforts were taken and the emissions of many precursors have been reduced in the last 10-20 years. Thereby in the typical summer smog situations the peak ozone concentrations could be reduced regionally (Oltmans et al., 2013). In the developing countries ozone concentrations increase Wang et al. (2009) due to the growing emission of ozone precursors.

Also in the tropics the trend varies regionally. Based on in situ measurements (1977-2002) Lelieveld et al. (2004) found an increase of $0.4\,\mathrm{ppb/yr}$ for the northern tropical Atlantic and slightly smaller increases between (0° and 20° S). The first one corresponds to roughly $2\,\mathrm{DU\,decade^{-1}}$ if the increase is constant up to 10 km altitude. An insignificant decline was found by Ziemke et al. (2005). They studied a combination of TOMS and SAGE ozone data between 1977 and 2003 over the Pacific Ocean. After extending the time series with OMI data up to 2010 (Ziemke and Chandra, 2012), they confirmed their results. From SCIAMACHY limb-nadir matching data (2002-2011) Ebojie et. al (2016) retrieved an insignificant positive trend for the tropics in general ($\approx 0.55\,\mathrm{DU\,decade^{-1}}$), but a significant trend of $\approx 4 \pm 1\,\mathrm{DU\,decade^{-1}}$ for southern central Africa. According to their data the tropospheric ozone column decreased on the South American west coast and the neighboring Pacific in the same order of magnitude. Beig and Singh (2007) used a combination of Nimbus 7 and the TOMS to retrieve a satellite based times series of TTOC (30°S to 30°N) between 1979 and 2005. According to their trend studies the tropospheric ozone burden increased by up to 7% especially over South-East Asia, and is transported westwards to Bay of Bengal and further to the Arabian Peninsular. Also over Central Africa and the southern tropical Atlantic they retrieved a significant positive trend. Over the Pacific Ocean no significant trend is found either from the satellite based TTOC (Beig and Singh, 2007) nor from in situ measurements (Oltmans et al., 2013).

We combine the time series of tropical tropospheric ozone, based on the CCD method, from four European satellites: GOME on ERS-2 (Burrows et al., 1999), SCIAMACHY on ENVISAT (Bovensmann et al., 1999), GOME-2 on MetOp-A (GOME-2A, Callies et al., 2000), GOME-2 on MetOp-B (GOME-2B) and the Finish-Dutch cooperation OMI (Levelt et al., 2006) flying on the AURA satellite. To get a consistent time series the data were harmonised at two important steps in the retrieval chain. The first harmonisation took place at beginning when the reflectances of the instruments were soft calibrated (Lerot et al., 2014), which led to good consistency between the L2 total columns from the individual instruments. Before combining the time series of the tropical tropospheric ozone column a second harmonisation corrected for different trends and biases in the TTOC data. The intermediate total ozone columns (TOZ) were not harmonised here. They were harmonised by Coldewey-Egbers et al. (2015). The differences in the TOZ between the sensors might also depend on the cloud fraction, which has not been considered during this harmonisation of the total columns.

For the first 7 years (1995 to 2002) only GOME data are available, there after the number of data increased with the launches of SCIAMACHY (2002), OMI (2004), GOME-2A (2007), and GOME-2B (2013). In 2003 the tape recorder on ERS-2 failed and only a limited number GOME data is available, during our retrieval these later data were usually ignored. ENVISAT lost contact in April 2012, therefore SCIAMACHY data were no longer received. AURA, MetOp-A and MetOp-B are still in service

Atmos. Meas. Tech. Discuss., doi:10.5194/amt-2016-139, 2016
Manuscript under review for journal Atmos. Meas. Tech.
Published: 3 June 2016

Atmospheric Measurement Techniques Discussions

so in principle data can be analysed until today. The OMI data are analysed until end of 2015. For the GOME-2 instruments the total ozone column are currently available until end of 2014. The algorithm described below is part of the operational processor for TROPOMI/S5P data retrieval, and the CCD based tropospheric ozone column will become operational for TROPOMI. After launch the TROPOMI TTOC will also be included in this time series.

The first section explains the data retrieval and some adaptions to the satellites used. It starts with a subsection on the underlying ozone column retrieval and introduces the CCD method to retrieve tropospheric columns before it finalizes with a small section on the results and the uncertainties. Before discussing long term trends we have to make sure that the different sensors measure comparable tropospheric ozone columns. Therefore the data are harmonised and compared to ozone sondes. Ozone sondes are common and standardized tool to measure atmospheric ozone worldwide. The paper concludes with the discussion of the TTOC trends including comparisons with previous trend studies.

2 Data Retrieval

The tropical tropospheric ozone columns were retrieved with the convective cloud differential (CCD) method. It was originally invented by Ziemke et al. (1998) and further improved by Valks et al. (2003, 2014). The CCD method retrieves the tropospheric column as difference between total ozone column (TOZ) and the stratospheric ozone column (SOC). It utilizes the processed total ozone columns and cloud data (level 2 data, Section 2.1) as retrieval input.

2.1 GODFIT Total ozone retrieval

A detailed description of the GODFITv3 algorithm is given in van Roozendael et al. (2012) or Lerot et al. (2014), here it is shortly summarized. The total ozone column data were generated in the framework of the ESA Climate Change Initiative-Ozone (CCI-Ozone) and are available at the CCI webpage: http://www.esa-ozone-cci.org (March 2016).

The GODFIT algorithm minimizes the difference between a sun normalized calculated earth shine spectrum and the observation between 325 and 335 nm using standard minimization tools. Therefore a linearized forward model is used with the state vector including the TOZ, a temperature shift, the effective surface albedo (polynomial 3rd order), the Ring-effect correction term, and an Earthshine Doppler shift. Among other variables the fit varies the TOZ which is then used to derive an ozone profile from a column classified ozone climatology (Bhartia., 2003) based on TOMS data. For the lowest altitude layers a better representation was found by replacing the TOMS data with the OMI/MLS tropospheric ozone climatology (Ziemke et al., 2011). Based on the ozone profile as well as the other atmospheric parameters (e.g. temperature profile) the radiative transfer model (LIDORT) calculates the intensity at the top of atmosphere as well as the Jacobian. During each minimization step the intensity has to be calculated.

The cloud fraction and cloud height are taken from cloud products calculated before from the same instruments. In the effective scene approach as proposed by Coldewey-Egbers et al. (2005) the effective altitude results from the cloud fraction weighted mean of the cloud top height and the ground altitude. The effective surface albedo is included in the GODFIT minimization retrieval. Even though the retrieval only includes the column above the effective surface, the total column still

Atmos. Meas. Tech. Discuss., doi:10.5194/amt-2016-139, 2016
Manuscript under review for journal Atmos. Meas. Tech.
Published: 3 June 2016

Atmospheric Measurement Techniques Discussions

represents the complete column including the troposphere. The final profile is integrated between the surface and the cloud altitude to calculate the ozone column below and inside the cloud (ghost column).

For GOME, SCIAMACHY, GOME-2A and GOME-2B the cloud data (altitude and cloud fraction) are taken from the FRESCO v6 algorithm (Wang et al., 2008), which is based on on the O_2 A-band. Due to the shorter spectral range the OMI cloud data are derived form O_2-O_2 absorptions at 477 nm. The cloud albedo is fixed at 0.8 in both cloud algorithms. For S5P the cloud data will be calculated using the OCRA/ROCINN algorithm, which is also based on the O_2 A-band (Schuessler et al., 2014; Loyola et al., 2010). The TROPOMI offline total ozone data product will be retrieved with the GODFIT algorithm.

Although the same algorithm was applied to GOME, SCIAMACHY and GOME-2A including the cloud algorithm, the total ozone columns of the three sensors deviated from each other, and possibly showed temporal drifts (Figure 7 in Lerot et al., 2014). Instrumental degradation (e.g. Coldewey-Egbers et al., 2008) cause errors in the absolute radiation of the level 1 data and thereby in the TOZ and the effective albedo retrieval. As a solution a soft calibration of the data was introduced. The measured spectra are compared to simulated spectra in the wavelength range between 325 and 335 nm. The simulated spectrum depends strongly on the ozone column, therefore for eight European stations Brewer ozone columns were included in the simulation of the respective spectra. Look up tables of reflectance corrections factors for the different sensors were build, which depend on the wavelength, the time and the solar zenith angle and the instrument viewing angle. The measured reflectance is multiplied with the correction factor, properly interpolated through the look up table.

A direct consequence of this soft calibration is to somehow align the retrieved ozone columns to the Brewer observations. In future versions a new calibration method based only on satellite observations is planned for the harmonisation of the total ozone columns.

To filter out outliers the total column data are rejected if rms fit-residuals exceeds an instrument dependent threshold. In total roughly 2% of the data were rejected.

2.2 Convective Cloud Differential Method for TROPOMI

The tropospheric ozone column will be operationally calculated from both the near real time and the offline total ozone columns for TROPOMI. The convective cloud differential algorithm summarized in the following originates from Valks et al. (2014). Compared to the original algorithm some improvements and adaptions to the GODFIT data have been made. The tropospheric columns can only be measured by satellites during cloud free observations. On the other hand this means that observations above high reaching clouds hardly contain any tropospheric signal. Therefore the measurements above high reaching clouds with a large cloud cover can be used to estimate the stratospheric column. For the retrieval of the total column (section 2.1) this effect is considered by adding a ghost column to the stratospheric signal. The ghost column is based on a climatology and includes the lowest part of the column, below as well as inside the cloud up to the effective cloud top height. Hence subtracting the ghost column from the total column results in the above cloud columnar ozone (ACCO):

$$ACCO = TOZ - ghost \tag{2}$$

Atmos. Meas. Tech. Discuss., doi:10.5194/amt-2016-139, 2016
Manuscript under review for journal Atmos. Meas. Tech.
Published: 3 June 2016

Atmospheric Measurement Techniques Discussions

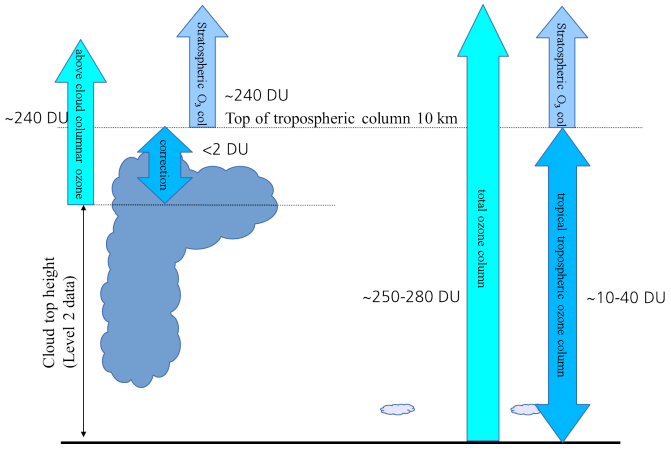

Figure 1. Sketch of the CCD method. The left side illustrates the estimate of the SOC using large convective clouds. In this case the cloud top is below 10 km, hence the correction column is subtracted. On the right the cloud free measurements of the total column and the TTOC are shown.

Compared to Valks et al. (2014) (eq. 3 therein) this is one adaption to the GODFIT data set and will also be used for offline tropospheric ozone columns from TROPOMI.

To determine the stratospheric ozone only clouds with a top height higher than 8.5 km are taken into account. Nevertheless the cloud top varies in a range between 8.5 km up to ≈ 15 km. The average cloud top height above 8.5 km in the current GODFIT dataset is close to 10 km, therefore the ACCO are normalized to 10 km (≈ 280 hPa). A climatology based correction column was added or subtracted depending on whether the cloud top was above or below the 10 km altitude level (Figure 1). For the ozone climatology we used the sonde based dataset by McPeters et al. (2007). The pressure altitude grid was interpolated to an altitude grid using the climatology from Fortuin and Kelder (1998). The correcting column is typically less than 1 DU. For GOME-2A (section 2.3) and January 2012 we checked the correction column in detail and found an average of -0.006± 0.196 DU, the extreme values were -2.626 DU and 7.314 DU.

The top height of 10 km is low for a tropospheric product, but shifting this altitude to higher levels only adds an offset which is given by the climatology profile between the higher altitude and the cloud top height. Even though the tropical stratosphere begins at roughly 17 km (≤ 100 hPa) we call the corrected ACCO stratospheric ozone column (SOC). The optimal top height for TROPOMI is currently under investigation but can hardly be fixed prior to the launch.

The SOC is determined over a clean reference area with a sufficient frequency of high convective clouds (70° E and 170° W Valks et al., 2014) and averaged over a certain period. For TROPOMI a temporal resolution of several days might be achieved. Thereby we assume that the stratospheric ozone column is constant in time and longitude. These assumptions are fulfilled only in the tropics, which limits the algorithm to a range of 20° S to 20° N. Due to the mitigation of the ITCZ the data are binned to latitude bands of 1.25° each.

Atmos. Meas. Tech. Discuss., doi:10.5194/amt-2016-139, 2016
Manuscript under review for journal Atmos. Meas. Tech.
Published: 3 June 2016

Atmospheric Measurement Techniques Discussions

A measurement pixel is cloud free if the cloud cover is less than 10%. The CCD method is sketched in Figure 1. Here the cloud free observations as well as the convective cloud measurements are shown simultaneously. On left the ACCO is shown as the ozone column above the effective cloud top height given by the cloud retrieval. The correction term between the cloud top height and the fixed level (10 km) is subtracted from the ACCO. The other part of the figure shows the cloud free case with less than 10% cloud fraction, the TTOC is the difference between the TOZ and the SOC:

$$TTOC = TOZ_{cloudfree} - SOC \tag{3}$$

The TTOCs and TOZs for cloud free pixels were averaged over the time period used for the SOC and regridded to $2.5° \times 1.25°$ resolution. Negative values in the averaged TTOCs were skipped. Due to the high resolution of the TROPOMI instrument and the expected large number of data points per grid cells we assume that the complete ground pixel is in the same grid box as the centre point.

One of the basic assumptions of the CCD method is that the stratospheric ozone column is constant along the latitude bands and for the respective time period. In the winter months this assumption is not always fulfilled on both hemispheres. Stratospheric intrusions cause local changes in the stratospheric columns, which sometimes results is misleading tropospheric ozone columns. Usually an automated quality control prevents this consequence for the TTOC. The quality control has four criteria for the stratospheric reference data to be good:

- The stratospheric column must not be lower than 200 DU.
- The number of observations in the stratospheric reference must be higher than a minimum threshold.
- The standard deviation in the stratospheric reference for the certain latitude band must be lower than a certain threshold.
- The gradient in the stratospheric reference must not exceed a certain maximum value ($\approx 5 DU/band$).

The thresholds depend on the instruments and will be adapted to the real measurements as soon as they are available. Currently default values are used based on the experiences gained in the data retrievals for the instruments mentioned below (section 2.3). In the final algorithm also the time resolution has to be considered. The standard deviation of the TTOC from the individual observations within a grid cell represents both the atmospheric inhomogeneity and the statistical error of the TTOC. Therefore it is an appropriate estimate of the error. The uncertainty in the TTOC from TROPOMI can be estimated based on the current instruments (section 2.3) to a range of $\approx$ 3 to 5 DU. The uncertainty does not to depend on the pixel size of the individual observers.

2.3 Adaption of the algorithm to current instruments

The algorithm as described in the previous section (2.2) was developed for the TROPOMI instrument on S5P. However, the launch is scheduled for October/November 2016, therefore the algorithm was applied to the data of the current European satellites: GOME, SCIAMACHY, OMI, GOME-2A and GOME-2B. All these instrument have a coarser resolution and less coverage. To some extend the algorithm had to be adapted to the different instruments. In a first step we reduced the temporal

Atmos. Meas. Tech. Discuss., doi:10.5194/amt-2016-139, 2016
Manuscript under review for journal Atmos. Meas. Tech.
Published: 3 June 2016

resolution from ≈ 6 days to 1 month. Which increases the number of data points per grid cell. On the other hand the assumption of a temporal stable stratospheric ozone column might not be valid.

In the tropics a grid cell of 2.5° longitude measures less than 280 km, hence it is smaller than a GOME pixel (≈ 320 km). In the latitudinal direction however, the pixels are by far smaller than the grid cells (≈ 40 km vs 139 km). Because of that during the regridding the GOME data are weighted with the longitudinal fraction inside a grid box. The OMI footprint is 13 km × 24 km and hence small enough to apply the original S5P algorithm without any weighting. The TTOCs differ by ≈ ±0.3 DU between the weighted and the non weighted averaging even for GOME-2A and SCIAMACHY. The small difference supports the application of the faster and easier operational averaging for also SCIAMACHY, GOME-2A and GOME-2B. Because for the stratosphere the column between 70° E and 170° W (120° or more than 13000 km) is averaged, the weighting is not useful at this point for any of the instruments.

It is obvious that the threshold for the number of observations per latitude band differs between OMI and GOME. Also the number of tropospheric columns per grid cell varies between the individual sensors, for OMI the maximum numbers are above 1000 for GOME the maximum sum of weights is usually between 40 and 60.

The standard deviation of the TTOC is lognormal distributed with mean values between 3.3 and 4.39, depending on the instrument. The width varies between 1.33 and 1.77. In the merged product (section 3) the propagated standard deviations of the individual sensors determine the final error to 3.8 ± 1.6 DU.

The algorithm was verified in the framework of the TROPOMI/S5P product development by a similar product from the University Bremen (Leventiduo et al., 2016). When applied to the same total ozone and cloud data, the difference between the two algorithms was typically less than 1 DU. A detailed error discussion based on the error propagation from the fits can be found in Leventiduo et al. (2016). While they apply the CCD retrieval to WFDOAS Ozone columns, our data are derived from the GODFITv3 total columns (section 2.1). Moreover the spatial resolution is 4 times coarser 5° × 2.5° compared to 2.5° × 1.25°. Due to these differences the total error is slightly higher than our estimates: 5 to 7 DU compared to ≈ 3.8 ± 1.6 DU.

2.4 CCD Results

The first results from TROPOMI are awaited by the end of 2016, until then we focus on the existing instruments. The TTOC above the tropical Atlantic is strongly influenced by the sources of ozone precursors which originate from central Africa and are transported westwards with the trade winds. The mitigation of the ITCZ over the African continent causes similar mitigation of the rain season and the burning season, when harvested fields or parts of the rainforests are burned. A respective change in the location of the ozone maximum is visible in figure 2. The figure shows the 20 years average tropospheric ozone distribution for December, January, February (DJF) and June, July, August (JJA) as well as the propagated standard deviations form monthly data. In JJA a clear ozone maximum on the central African coast is observed, in DJF when the burning season is further north, only moderated enhancement is observed there. A stronger maximum is found close to the South American coast and further south. This is probably caused biomass burning emissions from South America.

Over the central Pacific (150W to 150E) the TTOC reaches its minimum of less than 10 DU. In the same region also the standard deviation is low. Due to the quality control data at the winter edge of the tropics are often dismissed and only less data

Atmos. Meas. Tech. Discuss., doi:10.5194/amt-2016-139, 2016
Manuscript under review for journal Atmos. Meas. Tech.
Published: 3 June 2016

Atmospheric Measurement Techniques Discussions

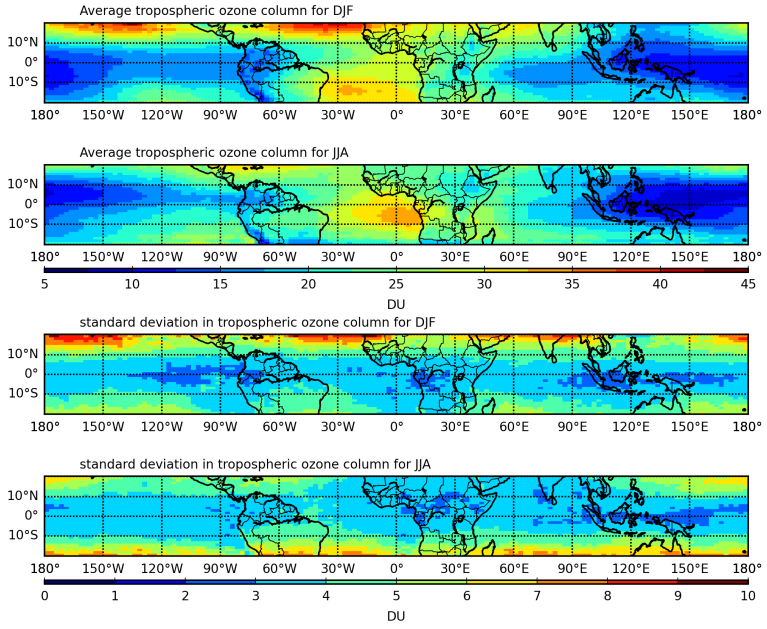

Figure 2. Top: Mean tropospheric ozone column for Dec.-Feb. and June-Aug. based on the merged CCD data set from all sensors for 1995 to 2015 (section 3). Bottom: Standard deviation of the tropospheric ozone column. Note the different colour bars for the TTOC and its deviation.

are considered in the averages and the deviations in figure 2. Moreover some of these data might just pass the quality check but are of limited quality. This causes the observed higher standard deviations towards the northern edge in the boreal winter and southern edge in the austral winter.

3 Harmonisation

The tropospheric ozone columns are harmonised to reduce instrumental effects in the long term time series. Thereby the different offsets and drifts of the instruments shall be reduced. We used SCIAMACHY as reference and compared the TTOC from the other instruments to this reference. SCIAMACHY has a good temporal overlap with the OMI, GOME-2A and GOME. Moreover the cloud data are based on the same algorithm as for GOME, GOME-2A and GOME-2B. The longitudinal and latitudinal averaged differences $< \Delta >_{(lat,long)}$ of the TTOCs between the other sensor ($inst$ in eq. 4) and the reference was approximated by a combination of the linear function and several sine and cosine functions with three different periods (1 year,

Atmos. Meas. Tech. Discuss., doi:10.5194/amt-2016-139, 2016
Manuscript under review for journal Atmos. Meas. Tech.
Published: 3 June 2016

Atmospheric Measurement Techniques Discussions

6 month and 4 month):

$$< TTOC_{inst} - TTOC_{SCIAMACHY} >_{(lat,long)} (t) = a + b \cdot t + \sum_{i=1}^{3} (c_i \cdot sin(\frac{2 \cdot \pi \cdot i \cdot t}{12}) + d_i \cdot cos(\frac{2 \cdot \pi \cdot i \cdot t}{12})) + r(t) \quad (4)$$

$$= cor(t) + r(t) \quad (5)$$

Where t is the time in month between January 1995 and December 2015, a, b, c_i and d_i are the fit parameters and r(t) is the residual structure. Wherever the fit coefficients were not robust ($> 2 \times \sigma$) they were set to zero. The respective correction function cor(t) was added to the TTOC(lat,long,t) for the complete tropics. This means that the difference between the original data set and the harmonised data set depends only on the time.

The extrapolation of the correction for the GOME data from 2002 to 2011 back to 1995 was too uncertain. Especially because the largest part of the time overlap between SCIAMACHY and GOME (2002-2011) is affected by the tape recorder failure of GOME. Therefore many GOME data in this period are at the northern edge of the tropics (15-20N), where the data retrieval is often uncertain (Section 2.4). As a consequence of that the number of common data points per month is low. If the data after 2003 are skipped, the overlapping period encompasses just one year of data (12 data points), this is not sufficient to fit any trend or even constant function. The GOME data are not harmonised to SCIAMACHY. For OMI the fit for the offset and the slope (a and b in eq. 4) were not robust, therefore we replaced the linear part of the harmonisation function (Figure 3) by the averaged differences. While for GOME and OMI no trend was found or allowed, the difference between SCIAMACHY and GOME-2A showed a strong increase in time 0.32 ± 0.04 DU per year. The reason for this trend is not yet fully understood. In the stratospheric reference column the trend was $-0.11 \pm 0.12\,\mathrm{DU\,decade^{-1}}$ when compared to the stratospheric column of the SCIAMACHY. The total columns agree well after the soft calibration is applied. However, in our data set only the cloud free observations are considered whereas Lerot et al. (2014) took all data into account. MetOp-B was launched into space in Sep. 2012, roughly half a year after the last SCIAMACHY data. So the GOME-2B data can not be harmonised to SCIAMACHY, directly. Therefore the harmonised GOME-2A and OMI act as reference for GOME-2B.

In the overlapping periods the harmonised TTOC agree very well with each other (table 1). The difference for all TTOC between the reference instrument SCIAMACHY and the other observers shows a small Gaussian distribution. The parameters do not change for GOME because here no correction was added. The fit improves slightly for OMI. Especially the bias between GOME-2A and SCIAMACHY is reduced.

The maximum differences given in table 1 or in figure 3 reach up to 2 DU. Relative to the tropospheric ozone column of roughly 20 to 40 DU the difference is 10 to 5%. In the time series of the TTOC the differences can be seen (figure 4). While in the original data set the OMI TTOC is always above the SCIAMACHY data and GOME-2A is most of the time below, the harmonised data agree better for all sensors. The observed difference between OMI and SCIAMACHY might also result from real atmospheric changes. The overpass times of the two satellites differ by more than 3 hour (10:00 LT to 13:30 LT), during this time of the day the tropospheric ozone burden usually increases. For the trend analysis and similar application it has to be corrected for but the harmonised data must not be used to study diurnal variations.

Atmos. Meas. Tech. Discuss., doi:10.5194/amt-2016-139, 2016
Manuscript under review for journal Atmos. Meas. Tech.
Published: 3 June 2016

Atmospheric Measurement Techniques Discussions

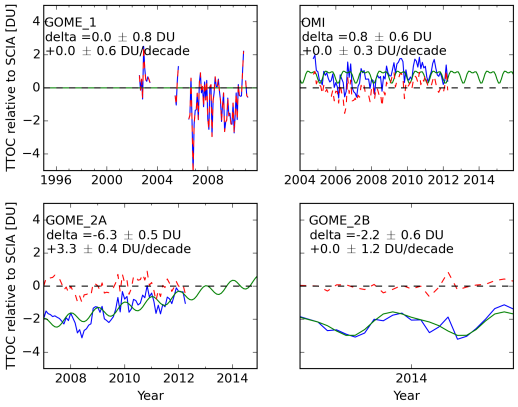

Figure 3. Average difference between the reference (SCIAMACHY) and the other sensors (blue), the fitted functions (cor(t)) in green and the difference to the harmonised data in red (r(t)).

Table 1. Parameters of Gaussian fits to the difference between the other instruments and the reference (SCIAMACHY). For GOME no correction was applied hence only one set of parameters is listed.

	bias	width	number
GOME	0.46	3.23	27784
OMI	0.79	2.69	326893
OMI(harmonised)	0.03	2.68	326893
GOME-2A	-1.43	2.62	232911
GOME-2A(harmonised)	0.00	2.55	232911
GOME-2B	-2.25	2.11	95113
GOME-2B(harmonised)	0.00	2.05	95113

We averaged the harmonised data of the individual instrument to a merged data product. For the first 7 years this product is identical with the GOME data. After July 2003 the GOME data are no longer considered in the merged data product as well as in the trend analysis below (section 4).

3.1 Comparison to Sondes

After the harmonisation we compared our results with integrated soundings from SHADOZ project Thompson et al. (2003) and the WOUDC (http://www.woudc.org/, March 2016).

The sonde data from the stations listed in table 2 were integrated up to 10 km (280 hPa) according to:

$$TTOC = k \cdot \sum (c_i(O_3) \cdot \delta P_i), \tag{6}$$

Atmos. Meas. Tech. Discuss., doi:10.5194/amt-2016-139, 2016
Manuscript under review for journal Atmos. Meas. Tech.
Published: 3 June 2016

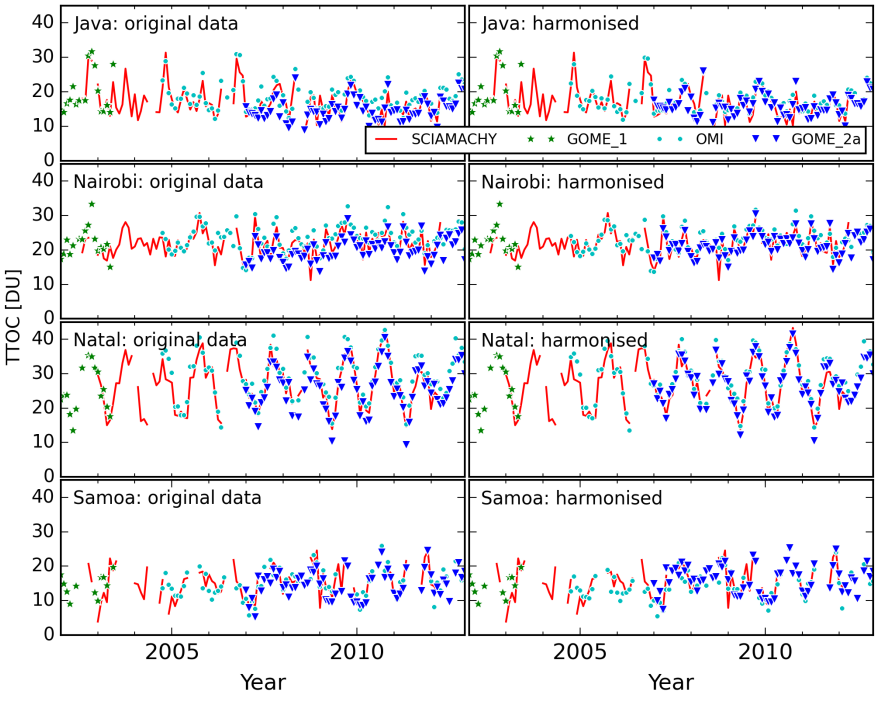

Figure 4. Time series of TTOC from SCIAMACHY as well as GOME, OMI and GOME-2A for SCIAMACHY life time at four selected sounding stations. Both the OMI and the GOME-2A data clearly deviate from the SCIAMACHY data in the original data (left), the deviation is reduced in the harmonised data (right).

where k=0.789, P is the pressure in hPa and c is the average ozone mixing ratio at the respective pressure level (http://www.temis.nl/data/fortuin.html, Feb. 2016). All sonde based TTOC per month are averaged. The sonde and the satellites are co located, when the sonde station is situated in the grid cell of the satellite data. For the comparison the difference between the sondes and satellite based TTOC were globally averaged and the same combination of linear and harmonic functions as in equation 4 was fitted to the difference.

For the complete period the merged data product shows only a small systematic trend compared to the sondes with $-0.29 \pm 0.3\,\mathrm{DU\,decade^{-1}}$ it is even smaller than the fitting error (figure 5). The trends relative to the sondes changes between +0.07 and -0.55 $\mathrm{DU\,decade^{-1}}$ when data of arbitrary sounding stations are skipped, in most cases it changed within the fitting errors of $\pm 0.3\,\mathrm{DU\,decade^{-1}}$.

The combined sounding network consists of 17 Stations around the tropics, with two stations being outside our latitude band (20° N or S). The satellite based TTOC is given at every grid cell (144×32). So the comparison is limited to a small selection of the satellites' data set, which is assumed to be representative for the complete set. Moreover the soundings take place once or twice per month, in a few exceptions up to four times. Up to daily observations form the satellites are averaged, depending on the local cloud cover. In the worst cases only one cloud free observation in a month is available. During the comparison

Atmos. Meas. Tech. Discuss., doi:10.5194/amt-2016-139, 2016
Manuscript under review for journal Atmos. Meas. Tech.
Published: 3 June 2016

Atmospheric Measurement Techniques Discussions

Table 2. SHADOZ and WOUDC stations used for the comparison with the satellite retrieved tropospheric columns. The two stations at the end of the table, are to close to the edges of the tropics, therefore they were not considered in the general comparison. However, they are mentioned for completeness. The first and last sondes included in the comparison are also listed, for 2015 only data from 5 stations are available.

Station	Longitude	Latitude	first sonde	last sonde
Java	111	-7.6	07-01-1998	30-10-2013
Singapore	103.8	1.3	18-01-2012	20-08-2014
Kuala Lumpur	101	2	15-01-1998	22-12-2014
Poona	73.8	18.5	04-01-1995	02-11-2011
Thiruvananthapuram	76.95	8.5	01-03-1995	28-12-2011
Nairobi	36.8	-1.3	04-12-1996	16-12-2015
Ascension Island	-14.4	-8	31-07-1997	24-08-2010
Natal	-35.4	-5.4	05-01-1998	24-09-2015
Paramaribo	-55.2	5.8	02-09-1999	29-12-2014
Costa Rica	-84	10.01	08-07-2005	18-12-2015
San Cristobal	-89.6	0.9	25-03-1998	30-01-2014
Papeete	-149.2	-18	31-07-1995	27-12-1999
Pago Pago (am. Samoa)	-170.6	14.4	08-08-1995	16-12-2015
Fiji	178.4	-18.1	26-02-1997	30-10-2013
Hawai	-155.04	19.4	04-01-1995	25-02-2015
Hanoi	105.8	21		
la Réunion	55.48	-21		

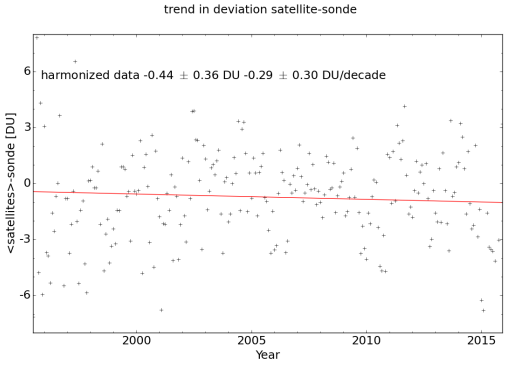

Figure 5. Difference between sondes and the merged data product.

Atmos. Meas. Tech. Discuss., doi:10.5194/amt-2016-139, 2016
Manuscript under review for journal Atmos. Meas. Tech.
Published: 3 June 2016

Atmospheric Measurement Techniques Discussions

this leads to a temporal mismatch which can hardly be reduced. Sondes measure along a vertical trajectory, the details of the trajectory depend on the local winds. A third uncertainty is introduced in the comparison because we have to assume that the TTOC in the respective grid cell is homogenous. Despite all these systematic uncertainties the data agree within a range of $\pm 5\,\mathrm{DU}$, which is comparable to the standard deviation of the satellite based TTOC (section 2.3).

4 Tropical tropospheric ozone trends

After the harmonisation the data of the instruments agree well with each other as well as with the ozone sondes, and the effects of different temporal drifts are minimized. This is an important requirement for the calculation of long term trends. For the following trend analysis we used the merged data set and calculated a global tropical trend as well as local trends. To reduce the noise in the local trends, the data were regridded to a $5^\circ \times 5^\circ$ grid. The fitting function consists of the same combination of linear term, sine and cosine functions as in eq. 4 in addition the indexes for the quasi biannual oscillation (QBO, http://www.esrl.noaa.gov/psd/data/correlation/qbo.data, Jan. 2016), for the El Niño (ENSO http://www.esrl.noaa.gov/psd/gcos_wgsp/Timeseries/Nino34/, Jan. 2016) and for the solar activity (The 10.7cm Solar Flux Data are provided as a service by the National Research Council of Canada, http://www.spaceweather.ca/solarflux/sx-5-mavg-en.php, Feb. 2016) were included. The indexes data were smoothed with a 3 month running average for ENSO and QBO and 7 month for the solar activity.

$$TTOC(lat, long, t) = a + b \cdot t + \sum_{i=1}^{3} (c_i \cdot sin(\frac{2 \cdot \pi \cdot i \cdot t}{12}) + d_i \cdot cos(\frac{2 \cdot \pi \cdot i \cdot t}{12})) + e \cdot ENSO_{3.4} + f \cdot QBO + g \cdot solar \qquad (7)$$

The coefficients a to g depend on latitude and longitude except for the tropical average. For most grid cells the QBO and the solar indexes turned out to be insignificant. The tropically averaged ozone increases by $0.75 \pm 0.12\,\mathrm{DU\,decade^{-1}}$ (figure 6).

Locally the trends vary between -0.8 and $1.8\,\mathrm{DU\,decade^{-1}}$. Figure 7 shows the fit for the case of the maximum trend (b in eq. 7). The data were observed on the African coast, in this region the effect of El Niño on the TTOC is low.

The times series has very pronounced annual cycle, with a peak to peak amplitude of about $10\,\mathrm{DU}$. The maximum in July/August coincides with maximum fire activity in southern Central Africa (e.g. https://firms.modaps.eosdis.nasa.gov/firemap/, Jan. 2016). The large forest fires emit the main ozone precursors ($\mathrm{NO_x}$ and VOCs). Both ozone and its precursors are transported westward with the trade winds, because of that the same annual cycle can be found far away in the Atlantic ocean (Figure 2).

The distribution of the increasing and decreasing trends (b in eq. 7) is indicated in figure 8. If the trend exceeds the $2 \times \sigma$ fit error, it is significant and the respective regions are marked with crosses.

Over central Africa and downwind over the Atlantic Ocean a positive trend is found, also in the central equatorial Pacific a significant positive is detected. Our results show a significant decrease over New Guinea extending to the east into the Pacific Ocean. The tropospheric ozone declines over the central America, although this trend is small and insignificant.

Atmos. Meas. Tech. Discuss., doi:10.5194/amt-2016-139, 2016
Manuscript under review for journal Atmos. Meas. Tech.
Published: 3 June 2016

Atmospheric Measurement Techniques Discussions

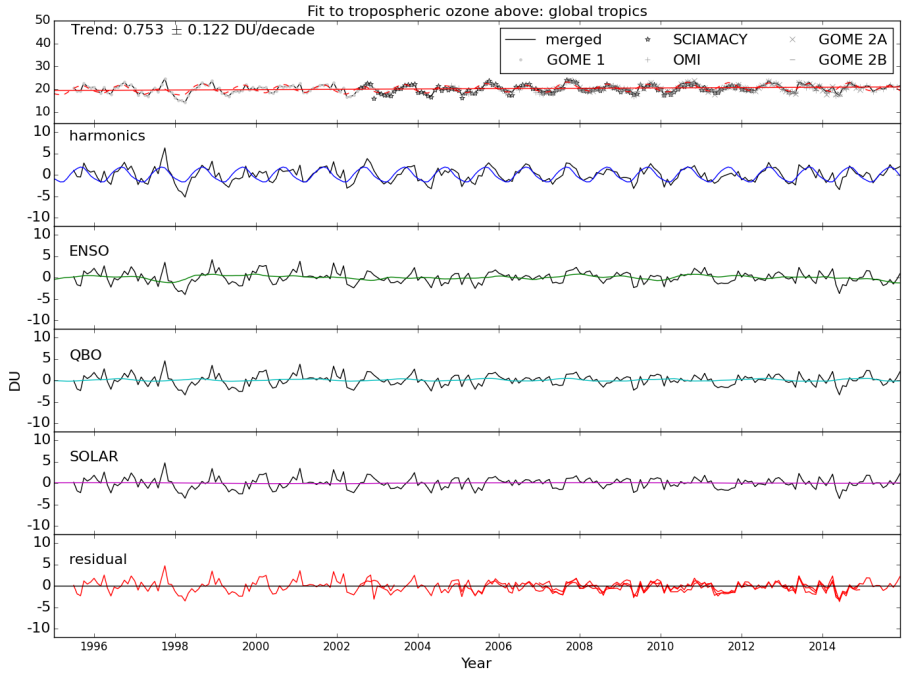

Figure 6. Fit of the tropically averaged tropospheric ozone columns for the years 1995 until 2015. Top: The merged data product with the fitted linear trend is shown, the individual instruments are shown for comparison. In the next panels the harmonic functions, and the indexes for ENSO, QBO and solar activity are shown. To illustrate the instrumental variance, the bottom panel displays the residuals for the individual instruments.

4.1 Seasonal Trends

Besides the over all trend the time series offers the possibility to study local or seasonal trends. The strong seasonal cycle for the TTOC over the African coast is visible in figure 7. In this region a strong increase is found. But whether this increase is caused by increasing fire emissions or by an increase in the background TTOC can hardly be explained with the figures above. In the overall trends the sine and cosine terms reflected the seasonal cycle, when focusing on the individual seasons this term must not be considered:

$$TTOC_{season}(lat, long, t) = a + b \cdot t + e \cdot ENSO_{3.4} + f \cdot QBO + g \cdot solar \quad (8)$$

Again the fit parameters depend on the longitude and latitude, but also global averages were fitted. Maps of the seasonal trend (b(lat,long) in eq. 8) can contribute to clarify this question (figure 9). According to this figure the main increase in central Africa is found in the burning season, indicating that over the years more fields and forests are burned.

For other regions like the Indian ocean the trends went in the opposite directions depending on the season. The TTOC decreased between September and February and increased strongly between March and May. Overall the seasonal trend maps are quite noisy compared to the general trend map. This effect might be caused by the still limited number of data (21 years

Atmos. Meas. Tech. Discuss., doi:10.5194/amt-2016-139, 2016
Manuscript under review for journal Atmos. Meas. Tech.
Published: 3 June 2016

Atmospheric Measurement Techniques Discussions

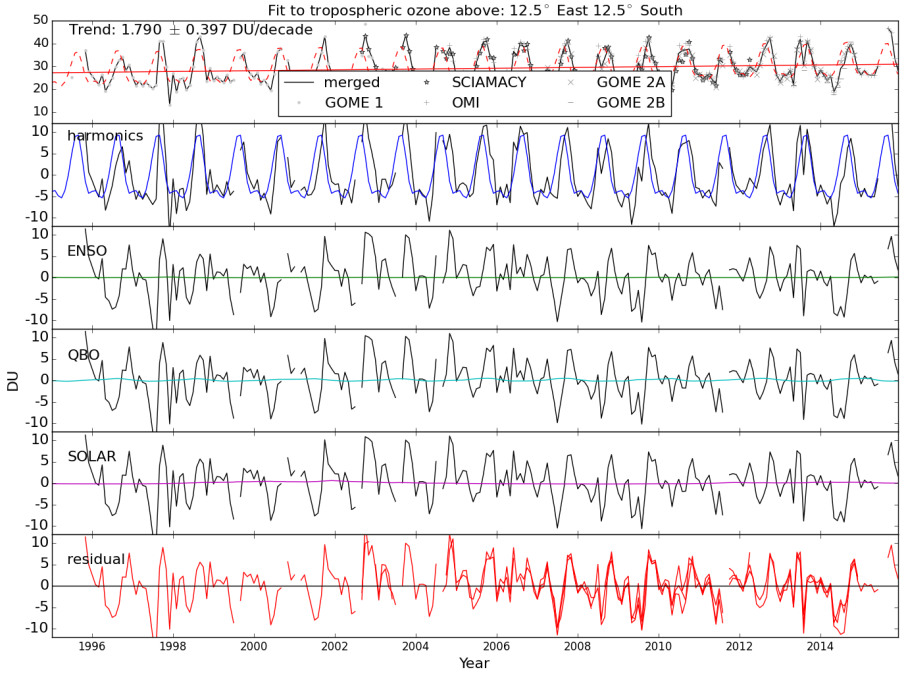

Figure 7. Similar to figure 6 for the trend in the grid box at 10-15° E and 10-15° S (African west coast). Here the maximum trend was observed. The time series is dominated by an annual cycle with a local ozone maximum in July / August.

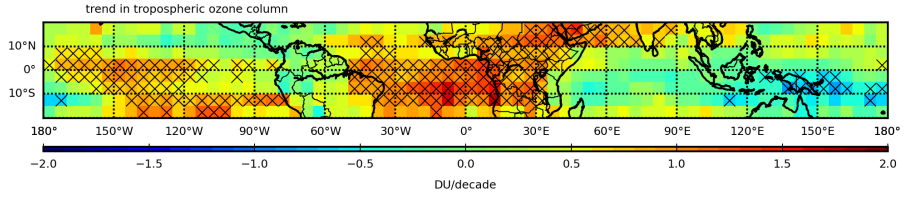

Figure 8. Tropical map of the tropospheric ozone trends. The crosses indicate regions where trends exceed the $2 \times \sigma$ fit error. Overall the tropospheric ozone increased in the last 20 years. Only for New Guinea and the neighboring Pacific Ocean a significant decrease is found.

Atmos. Meas. Tech. Discuss., doi:10.5194/amt-2016-139, 2016
Manuscript under review for journal Atmos. Meas. Tech.
Published: 3 June 2016

Atmospheric Measurement Techniques Discussions

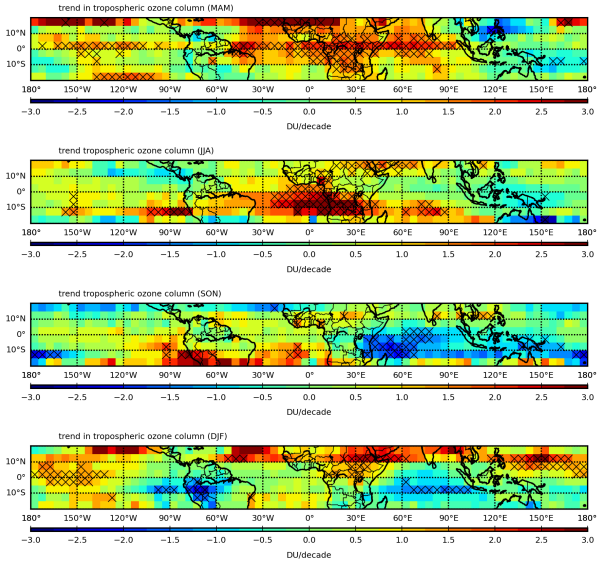

Figure 9. Same map as in Figure 8 but for the different seasons, mind the different scales. The main increase over southern Central Africa and the Atlantic Ocean is found in June to August, which is the burning season in southern Central Africa.

$\times$ 3 month = 63 data points in the maximum). The seasonal global average trends vary between $0.74 \pm 0.85\,\mathrm{DU\,decade^{-1}}$ in MAM and $0.25 \pm 0.93\,\mathrm{DU\,decade^{-1}}$ in JJA. For all seasons the global fits are not robust as the fitted trends are less than the respective error.

5 Conclusions

Based on the GODFIT L2 ozone data from GOME, SCIAMACHY, OMI, GOME-2A and GOME-2B we generated a harmonised data set of tropical tropospheric ozone columns for the period 1995 to 2015. In the overlapping periods the TTOC from the different sensors agree very well. The TTOC showed a global averaged increas of $0.75\,\mathrm{DU\,decade^{-1}}$. Large trends were observed over the African continent and over the Atlantic ocean, with a maximum trend of $1.79\,\mathrm{DU\,decade^{-1}}$ on the African Atlantic coast. Also Ebojie et. al (2016) and Beig and Singh (2007) observed an increase in tropospheric ozone in this region for the years 2002-2012 ($4\,\mathrm{DU\,decade^{-1}}$) and 1979-2005 ($2\%\,\mathrm{decade^{-1}} \approx 6\,\mathrm{DU\,decade^{-1}}$) respectively. In both cases the respective region was smaller than in this study.

Due to the economic growth and the accompanying growing emissions we expected a stronger positive trend in South East Asia. This was partly found in the SCIAMACHY limb nadir matching data Ebojie et. al (2016), and much stronger in the TOMS observation Beig and Singh (2007) . Ziemke et al. (2005) averaged TOMS CCD data for the Pacific Ocean (120° E to 120° W). They found an almost insignificant decline ($\approx 1\,\mathrm{DU\,decade^{-1}}$) for 1979 to 2005 between 0° and 15° N. South of the Equator the TTOC showed no trend. This partly contradicts our findings of a positive trend over large parts of the Pacific, at least for the northern part were no negative trend is found. In the south both positive and negative trends may add

Atmos. Meas. Tech. Discuss., doi:10.5194/amt-2016-139, 2016
Manuscript under review for journal Atmos. Meas. Tech.
Published: 3 June 2016

Atmospheric Measurement Techniques Discussions

to zero. For American Samoa (14.5°S 170.6°E) Oltmans et al. (2013) measured an insignificant positive trend of 0.02 ± 0.34 $\mathrm{ppb/year}$ ($\approx 0.1 \pm 1.7\,\mathrm{DU\,decade^{-1}}$ between 1991 and 2010, whereas our trend for this region was negative (-0.75 $\pm$ 0.3 $\mathrm{DU\,decade^{-1}}$).

The global tropical trend is $0.75\,\mathrm{DU\,decade^{-1}}$ according to this study, for the SCIAMACHY data Ebojie et. al (2016) $\approx 0.55\,\mathrm{DU\,decade^{-1}}$ can be estimated. With respect to the differences in the distribution pattern this agreement is very good.

The data set will be extended as soon as new OMI, GOME-2A or GOME-2B total columns have been processed. After the launch of the Sentinel 5 Precursor mission (October/November 2016) also TROPOMI columns will be included. In this way the TTOC data record will be extended for at least the 7 years S5P nominal mission and this will allow the monitoring of future trends in the tropical ozone. Additionally the TTOC time series will be continued with the future Sentinel 5 mission. The extension will result in more reliable trend data, maybe also a temporal change in the trend might be resolved.

The harmonised TTOC data will soon be available on the ozone CCI webpage (http://www.esa-ozone-cci.org, April. 2016).

Acknowledgements. Financial support was given by the Bayerisches Staatsministerium für Wirtschaft und Medien, Energie und Technologie (grant 07 03/893 73/ 5 /2013). The retrieval was developed with the grand provided in preparation for the Sentinel 5 Precursor mission. The TTOC harmonisation has been performed as part of ESA's Climate Change Initiative -Ozone project. We thank ESA for providing the GOME, SCIAMACHY and EUMETSAT for the GOME-2 (A and B) level 1 satellite data. We acknowledge the use of Level 1 data from Aura-OMI from NASA/KNMI. We thank the different national and international funding agencies for supporting the ozone soundings in the SHADOZ network and for providing data to the WOUDC. The World Ozone and Ultraviolet Radiation Data Centre and the SHADOZ project make the routine sonde data accessible.

Atmos. Meas. Tech. Discuss., doi:10.5194/amt-2016-139, 2016
Manuscript under review for journal Atmos. Meas. Tech.
Published: 3 June 2016

References

Bhartia, P. Algorithm Theoretical Baseline Document, TOMS v8 Total ozone algorithm. available at: http://toms.gsfc.nasa.gov/version8/version8_update.html, 2003.

Beig, G., and V. Singh: Trends in tropical tropospheric column ozone from satellite data and MOZART model, Geophys. Res. Lett., 34, L17801, doi:10.1029/2007GL030460, 2007.

Bovensmann, H., Burrows, J. P., Buchwitz, M., Frerick, J., Noel, S., Rozanov, V. V., Chance, K. V., and Goede, A. P. H.: SCIAMACHY: mission objectives and measurement modes, J. Atmos. Sci., 56, 127-150, doi:10.1175/1520-0469(1999)056<0127:SMOAMM>2.0.CO;2, 1999.

Burrows, J.P., Weber, M., Buchwitz, M., Rozanov, V. V., Ladstätter-Weißenmayer, A., Richter, A., de Beek, R., Hoogen, R., Bramstedt, K., Eichmann, K.-U., Eisinger, M., and Perner, D.: The Global Ozone Monitoring Experiment (GOME): mission concept and first scientific results, J. Atmos. Sci., 56, 151-175, doi:10.1175/1520-0469(1999)056<0151:TGOMEG>2.0.CO;2, 1999.

Callies, J., Corpaccioli, E., Eisinger, M., Hahne, A., and Lefebvre, A.: GOME-2 – Metop's second generation sensor for operational ozone monitoring, ESA Bull.-Eur. Space, 102, 28-36, available at: http://www.esa.int/esapub/bulletin/bullet102/Callies102.pdf, 2000.

Coldewey-Egbers, M., Weber, M., Lamsal, L.N., de Beek, R., Buchwitz, M., and Burrows, J. P.: Total ozone retrieval from GOME UV spectral data using the weighting function DOAS approach, Atmos. Chem. Phys., 5, 1015-1025, doi:10.5194/acp-5-1015-2005, 2005

Coldewey-Egbers, M., Slijkhuis, S., Aberle, B., and Loyola, D.: Long-term analysis of GOME in-flight calibration parameters and instrument degradation, Appl. Opt., 47(28), 4749-4761, doi:10.1364/AO.47.004749, 2008.

Coldewey-Egbers, M., Loyola, D. G., Koukouli, M., Balis, D., Lambert, J.-C., Verhoelst, T., Granville, J., van Roozendael, M., Lerot, C., Spurr, R., Frith, S. M., and Zehner, C.: The GOME-type Total Ozone Essential Climate Variable (GTO-ECV) data record from the ESA Climate Change Initiative, Atmos. Meas. Tech., 8, 3923-3940, doi:10.5194/amt-8-3923-2015, 2015.

Cooper, O. R., Parrish, D. D., Ziemke, J., Balashov, N. V., Cupeiro, M., Galbally, I. E., Gilge, S., Horowitz, L., Jensen, N. R., Lamarque, J.-F., Naik, V., Oltmans, S. J., Schwab, J., Shindell, D. T., Thompson, A. M., Thouret, V., Wang, Y., and Zbinden, R. M.: Global distribution and trends of tropospheric ozone: An observation-based review, Elem. Sci. Anthr., 2, 000029, doi:10.12952/journal.elementa.000029, 2014.

Ebojie, F., Burrows, J. P., Gebhardt, C., Ladstätter-Weißenmayer, A., von Savigny, C., Rozanov, A., Weber, M., and Bovensmann, H.: Global tropospheric ozone variations from 2003 to 2011 as seen by SCIAMACHY, Atmos. Chem. Phys., 16, 417-436, doi:10.5194/acp-16-417-2016, 2016.

Feng, Z., and Kobayashi, K.: Assessing the impacts of current and future concentrations of surface ozone on crop yield with meta-analysis, Atmospheric Environment 43, 1510-1519, doi:10.1016/j.atmosenv.2008.11.033, 2009.

Fishman, J. and Larsen, J. C.: Distribution of total ozone and stratospheric ozone in the tropics: Implications for the distribution of tropospheric ozone, J. Geophys. Res., 92, 6627-6634, 1987.

Fortuin, P. J. F. and Kelder, H.: An ozone climatology based on ozonesonde and satellite measurements, J. Geophys. Res., 103(D24), 31709-31734, doi:10.1029/1998JD200008, 1998.

Lelieveld, J., van Aardenne, J., Fischer, H., de Reus, M., Williams, J., and Winkler, P.: Increasing ozone over the Atlantic Ocean, Science, 304(5676), 1483-1487, 2004.

Lerot, C., van Roozendael, M., Spurr, R., Loyola, D., Coldewey-Egbers, M., Kochenova, S., van Gent, J., Koukouli, M., Balis, D., Lambert, J.-C., Granville, J. and Zehner, C.: Homogenized total ozone data records from the European sensors GOME/ERS-2, SCIAMACHY/Envisat and GOME-2/MetOp-A. J. Geophys. Res., 119, 3, 1639-1662, doi:10.1002/2013JD020831, 2014.

Levelt, P. F., van den Oord, G. H. J., Dobber, M. R., Mälkki, A., Visser, H., de Vries, J., Stammes, P., Lundell, J. O. V., and Saari, H.: The ozone monitoring instrument, IEEE T. Geoscience and Remote Sensing, 44, 1093-1101, doi:10.1109/TGRS.2006.872333, 2006.

Leventidou, E., Eichmann, K.-U., Weber, M., and Burrows, J. P.: Tropical tropospheric ozone columns from nadir retrievals of GOME-1/ERS-2, SCIAMACHY/Envisat, and GOME-2/MetOp-A (1996-2012), Atmos. Meas. Tech. Discuss., doi:10.5194/amt-2015-401, in review, 2016.

Loyola D., Thomas W., Spurr, R., and Mayer, B.: Global patterns in daytime cloud properties derived from GOME backscatter UV-VIS measurements, International Journal of Remote Sensing, 31, 16, 4295-4318, doi: 10.1080/01431160903246741, 2010.

McPeters, R. D., G. J. Labow, and J. A. Logan, Ozone climatological profiles for satellite retrieval algorithms, J. Geophys. Res., 112, D05308, doi:10.1029/2005JD006823, 2007.

Nawrot, T., Nemmar, A. , and Nemery, B.: Update in Environmental and Occupational Medicine 2005, American Journal of Respiratory and Critical Care Medicine, Vol. 173, No. 9 , pp. 948-952. doi: 10.1164/rccm.2601010, 2006

Oltmans,S.J., Lefohn, A.S., Shadwick, D., Harris, J.M., Scheel, H.E., Galbally, I., Tarasick, D.W., Johnson, B.H., Brunke, E.-G., Claude, H., Zeng, G., Nichol, S., Schmidlin, f., Davies, J., Cuevas, E., Redondas, A., Naoe, H., Nakano, T. and Kawasato,T.: Recent tropospheric ozone changes - A pattern dominated by slow or no growth, Atmospheric Environment, Volume 67, Pages 331-351, ISSN 1352-2310, doi:10.1016/j.atmosenv.2012.10.057 ,2013.

van Roozendael, M., Spurr, R., Loyola, D., Lerot, C., Balis, D., Lambert, J.-C., Zimmer, W., van Gent, J., van Geffen, J., Koukouli, M., Granville, J., Doicu, A., Fayt C., and Zehner C.: Sixteen years of GOME/ERS-2 total ozone data: The new direct-fitting GOME Data Processor (GDP) version 5 Algorithm description, J. Geophys. Res., 117, D03305, doi:10.1029/2011JD016471, 2012.

Schuessler, O., Loyola, D., Doicu, A., and Spurr, G.: Information Content in the Oxygen A-band for the Retrieval of Macrophysical Cloud Parameters, IEEE Trans. Geosci. Remote Sens., 52(6), doi:10.1109/TGRS.2013.2271986, 2014.

Spurr, R., Natraj, V., Lerot, C., van Roozendael, M., and Loyola D.: Linearization of the Principal Component Analysis method for radiative transfer acceleration: Application to retrieval algorithms and sensitivity studies. J. Quant. Spectrosc. Radiat. Transfer 125,1-17, doi:10.1016/j.jqsrt.2013.04.002, 2013

Thompson, A.M., Witte, J.C., McPeters, R.D., Oltmans, S.J., Schmidlin, F.J., Logan, J.A., Fujiwara, M., Kirchhoff, V.W.J.H., Posny, F., Coetzee, G.J.R., Hoegger, B., Kawakami, S., Ogawa, T., Johnson ,B.J., Vömel, H., and Labow, G.: Southern Hemisphere Additional Ozonesondes (SHADOZ) 1998-2000 tropical ozone climatology 1. Comparison with Total Ozone Mapping Spectrometer (TOMS) and ground-based measurements, J. Geophys. Res., Vol. 108 No. D2, 8238, doi: 10.1029/2001JD000967, 2003.

Valks, P. J. M., Koelemeijer, R. B. A., van Weele, M., van Velthoven, P., Fortuin, J. P. F., and Kelder, H.: Variability in tropical tropospheric ozone: Analysis with Global Ozone Monitoring Experiment observations and a global model, J. Geophys. Res., 108, 4328, doi:10.1029/2002JD002894, 2003.

Valks, P., Hao, N., Gimeno Garcia, S., Loyola, D., Dameris, M., Jöckel, P., and Delcloo, A.: Tropical tropospheric ozone column retrieval for GOME-2, Atmos. Meas. Tech., 7, 2513-2530, doi:10.5194/amt-7-2513-2014, 2014.

Wang, P., Stammes, P., van der A, R., G. Pinardi, G., and van Roozendael, M.: FRESCO+: An improved O2 A-band cloud retrieval algorithm for tropospheric trace gas retrievals, Atmos. Chem. Phys., 8, 6565-6576, doi:10.5194/acp-8-6565-2008, 2008.

Wang, T., Wei, X. L., Ding, A. J., Poon, C. N., Lam, K. S., Li, Y. S., Chan, L. Y., and Anson, M.: Increasing surface ozone concentrations in the background atmosphere of Southern China, 1994-2007, Atmos. Chem. Phys., 9, 6217-6227, doi:10.5194/acp-9-6217-2009, 2009.

Ziemke, J. R., Chandra, S., and Bhartia, P. K.: Two new methods for deriving tropospheric column ozone from TOMS measurements: The assimilated UARS MLS/HALOE and convective-cloud differential techniques, J. Geophys. Res., 103, 22115-22127, 1998.

Atmos. Meas. Tech. Discuss., doi:10.5194/amt-2016-139, 2016
Manuscript under review for journal Atmos. Meas. Tech.
Published: 3 June 2016

Atmospheric Measurement Techniques Discussions

Ziemke, J. R., Chandra, S., and Bhartia, P. K.: A 25-year data record of atmospheric ozone from TOMS Cloud Slicing: Implications for trends in stratospheric and tropospheric ozone, J. Geophys. Res., 110, D15105, doi:10.1029/2004JD005687, 2005.

Ziemke, J. R., Chandra, S., Labow, G. J., Bhartia, P. K., Froidevaux, L., and Witte, J. C.: A global climatology of tropospheric and stratospheric ozone derived from Aura OMI and MLS measurements, Atmos. Chem. Phys., 11, 9237-9251, doi:10.5194/acp-11-9237-2011, 2011.

Ziemke, J. R. and Chandra, S.: Development of a climate record of tropospheric and stratospheric column ozone from satellite remote sensing: evidence of an early recovery of global stratospheric ozone, Atmos. Chem. Phys., 12, 5737-5753, doi:10.5194/acp-12-5737-2012, 2012.